Nanoscale

Accepted Manuscript

This article can be cited before page numbers have been issued, to do this please use: Q. Wang, J. Chen, H. Zhang, W. Wu, Z. Zhang and S. Dong, *Nanoscale*, 2018, DOI: 10.1039/C8NR06162A.

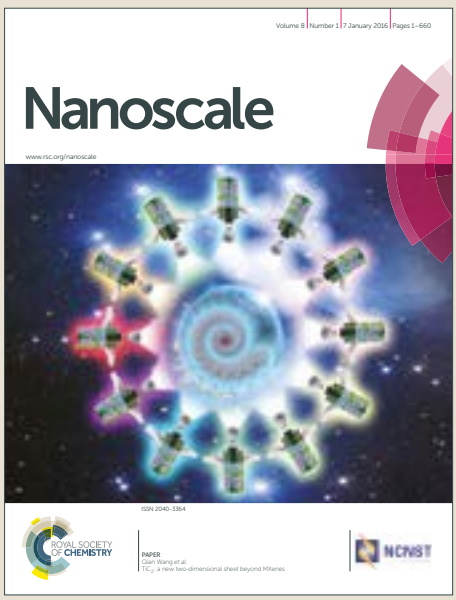

View Article Online
DOI: 10.1039/C8NR06162A

Journal Name

ARTICLE

Porous Co_3O_4 nanoplates with pH-switchable peroxidase- and catalase-like activity

Received 00th January 20xx,
Accepted 00th January 20xx

DOI: 10.1039/x0xx00000x

www.rsc.org/

Qingqing Wang,[a,b] Jinxing Chen,[a] He Zhang,[a] Weiwei Wu,[a] Zhiquan Zhang*[b] and Shaojun Dong*[a]

Porous Co_3O_4 nanoplates were synthesized via a soft template method. By using amphiphilic block copolymer F127 colloids as the pore producer, porous $Co(OH)_2$ nanoplates were prepared. After the procedure of annealing, the obtained Co_3O_4 reserved the hexagonal shape and similar size to the $Co(OH)_2$ precursor. The as-prepared porous Co_3O_4 nanoplates named Co_3O_4-F simultaneously possessed peroxidase and catalase mimetic activities. Interestingly, these two kinds of mimetic enzyme activities could be switched by pH. Meanwhile, temperature and the concentrations of Co_3O_4-F had a significance effect on the switch pH and the dual-enzyme mimetic catalytic ability. Moreover, Co_3O_4-F exhibited good peroxidase-like catalytic activity even in the neutral pH system, providing a new strategy for one-step analysis of glucose. A novel one-step colorimetric glucose biosensor was fabricated based on the Co_3O_4-F nanozyme, making the operation of detection simpler and easier.

Introduction

Nanozymes, nanomaterials with enzyme-like catalytic activities, have developed very fast since the first exciting discovery of Fe_3O_4 nanoparticles with unexpected peroxidase mimetic activity.[1] To date, various types of nanozymes have been found ranging from metal,[2, 3] metal oxide,[4, 5] metal coordination complexes[6, 7] to carbon-based nanomaterials,[8, 9] exhibiting oxidase, peroxidase, catalase (CAT) or superoxide dismutase (SOD) mimetic activity. Particularly, some nanozymes have possessed several kinds of mimetic catalytic properties simultaneously.[3, 10-12] Qu's group has demonstrated that MnO_2 possessed inherent SOD and CAT mimic activities. MnO_2 nanozymes were used as cytoprotective shells for yeast cells to enhance the cellular tolerance against severe physical stressors.[13] Besides, by combining V_2O_5 nanowire served as a glutathione peroxidase mimic, they constructed a multi-nanozymes cooperative platform V_2O_5@pDA@MnO_2 nanocomposite to mimic intracellular antioxidant enzyme-based defense system.[14] Futhermore, it was found that Mn_3O_4 nanozyme could simultaneously mimic those mentioned three antioxidant enzymes (SOD, CAT and glutathione peroxidase), providing efficient cytoprotection in a Parkinson's disease model.[15]

The mixed oxidation states of the metal in the nanozymes were considered to be the significant reason for the multi-enzyme mimetic activity.[15] For example, in the presence of mixed valence states of Ce^{3+} and Ce^{4+}, as well the oxygen vacancies, CeO_2 has the superoxide-scavenging activity,[16-18] and could efficiently catalyze the hydrolysis of nerve agents,[19] acting as the SOD nanozyme and phosphotriesterase mimetic hotspots, respectively. Moreover, CeO_2 also exhibits oxidase,[20-22] peroxidase[23] and CAT[24] mimetic activities, applied widely in the field of biosensing and biomedicine.[20-23, 25, 26] Since one nanozyme could possess multi-enzyme mimetic catalytic activity, however, there are few reports to discuss how to switch each kind of nanozyme's catalytic activity, which would be a great challenge in the way of developing nanozyme.

Here, we successfully synthesized porous Co_3O_4 nanoplates by using F127 colloids as the soft templates (Co_3O_4-F), which were found to exhibit both peroxidase-like and CAT-like activities. Importantly, we studied the switch conditions between the dual enzyme-like activity of Co_3O_4-F in detail.

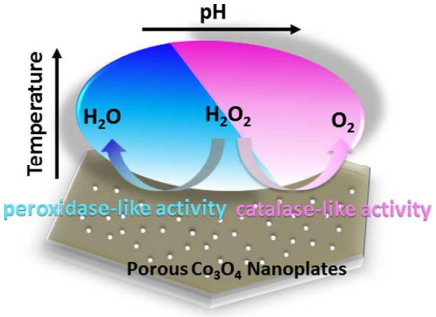

Scheme 1 Schematic presentation of porous Co_3O_4 nanoplates with temperature- and pH-switchable peroxidase- and CAT-like activity.

[a] State Key Laboratory of Electroanalytical Chemistry, Changchun Institute of Applied Chemistry, Chinese Academy of Sciences, Changchun, 130022, P. R. China
E-mail: dongsj@ciac.ac.cn (S. Dong), Tel: +86 431 85692886. Fax: +86 431 85689711
[b] College of Chemistry, Jilin University, Changchun, 130012, P. R. China
E-mail: zzq@jlu.edu.cn (Z. Zhang)
Electronic Supplementary Information (ESI) available: SEM images, kinetic studies on the peroxidase-like activity of Co_3O_4-F. See DOI: 10.1039/x0xx00000x

View Article Online
DOI: 10.1039/C8NR06162A

Nanozyme would like to exhibit CAT mimetic activity under the basic solution or with high concentration of Co_3O_4-F. The dual enzyme-like activity is dependent on the combined effect of pH and temperature in the reaction system. As shown in **Scheme 1**, with increasing of temperature, the dual enzyme mimetic activity of Co_3O_4-F was both enhanced. Meanwhile, even in the acid system nanozyme exhibited CAT-like activity and the optimal reaction pH for Co_3O_4-F as peroxidase mimic went towards lower pH. As a result, by modulating the optimal reaction conditions, a novel one-step colorimetric glucose biosensor was fabricated based on the peroxidase-like activity of Co_3O_4-F.

Experimental

Materials and chemicals

Pluronic® F127, Pluronic® P123, 3, 3', 5, 5'-tetramethylbenzidine (TMB) and glucose oxidase (GOx, from Aspergillus niger, 50 KU, 128.2 KU g^{-1}) were purchased from Sigma-Aldrich. Ammonia solution (NH_3, 25%), $Co(NO_3)_2{\cdot}6H_2O$, glucose, fructose, maltose, lactose and sucrose were obtained from Beijing Chemical Reagent Company (Beijing, China). All the chemicals were of analytical grade and used without further purification. Ultrapure water (≥18.2 MΩ cm) was used throughout the study.

Apparatus

UV/Vis absorption measurements were made on a Cary 500 UV-Vis-NIR spectrometer (Varian). Scanning electron microscopy (SEM) experiments were made on a PHILIPS XL-30 field-emission scanning electron microscope with an accelerating voltage of 10 kV. Transmission electron microscopy (TEM) measurements were performed on a JEM-2100F high-resolution transmission electron microscope operating at 200 kV. X-ray diffraction (XRD) patterns were obtained from a D8 ADVANCE (Bruker, Germany) X-ray diffractometer with Cu Kα radiation (λ = 1.5406 Å).

Preparation of porous Co_3O_4 nanoplates

In a typical procedure, 1 g Pluronic F127 and 0.25 g $Co(NO_3)_2{\cdot}6H_2O$ were respectively dissolved in 50 mL deionized water. Then, the mixture solution was stirred and heated to 80 °C by a water bath. Subsequently, 0.75 mL ammonia solution was added into the above solution. The whole mixture was stirred at 80 °C for another 1 h. The product was collected by centrifugation at 5000 rpm and washed thoroughly with deionized water several times. After drying at 60 °C, the obtained product named $Co(OH)_2$-F was calcined at 450 °C for 2 h under air with a heating rate of 2°C min^{-1} to form the porous Co_3O_4 nanoplates (Co_3O_4-F).

According to the above method, $Co(OH)_2$-P and Co_3O_4-P were synthesized by replacing Pluronic F127 with P123. In the case of $Co(OH)_2$ and Co_3O_4, a similar procedure was applied except for adding any soft template.

•OH radical measurement

0.625 mM terephthalic acid dissolved in 0.1 M HAc-NaAc buffer (pH 6.0), 50 mM H_2O_2 and different concentrations of Co_3O_4-F were first incubated at room temperature for 3 h, then the solutions were used for the measurement of OH radical carried out on Fluoromax-4 spectrofluorometer (Horiba Jobin Yvon Inc., France).

Steady-State kinetic analysis of Co_3O_4-F as peroxidase mimetics

Kinetic experiments were carried out in a reaction volume of 1.0 mL HAc-NaAc buffer solution (0.1 M, pH 6.0) containing 10 μg mL^{-1} Co_3O_4-F, 2 mM H_2O_2 and 0.25 mM TMB as substrate, unless otherwise stated. The mixture solutions were incubated at room temperature for 10 min and then used for absorbance measurement at wavelength 652 nm. The Michaelis-Menten constant was calculated using a Lineweaver-Burk plot: $1/V = K_m/V_m\ (1/[S] + 1/K_m)$, where V is the initial velocity, V_m is the maximal reaction velocity, [S] corresponds to the substrate concentration, and K_m is the Michaelis-Menten constant.

One-step colorimetric detection of glucose based on Co_3O_4-F peroxidase mimic

Glucose detection was performed as follows: 50 μL GOx (5 mg mL^{-1}), 10 μL Co_3O_4-F (1 mg mL^{-1}) and 200 μL of different concentrations of glucose in 0.1 M HAc-NaAc buffer solution (pH 6.0) were incubated at 25 °C for 30 min, and then used for absorbance measurement at wavelength 652 nm.

Results and discussion

Preparation and characterization of porous Co_3O_4 nanoplates

Pluronic® F127 (EO100-PO65-EO100) and Pluronic® P123 (EO20-PO70-EO20), the common amphiphilic triblock polymer which can self-assemble to micelles, have been applied widely in drug release[27, 28] and preparation of various porous materials as the pore producer.[29, 30] When the polymer concentration reaches the critical micelle concentration, F127 and P123 can form the spherical micelles owing to the plenty of hydrophobic and hydrophilic groups. In aqueous solution, Co^{2+} coordinates with water to form $[Co(H_2O)_6]^{2+}$, which can absorb to the external hydrophilic groups of the micelles to form a composite micelles mixed with $[Co(H_2O)_6]^{2+}$.[31] When aqueous ammonia is added, $Co(OH)_2$ is formed [eq.1] during the precipitation process, and porous $Co(OH)_2$ nanoplates can be obtained after a washing process. As shown in Fig. 1a and 1b, $Co(OH)_2$ nanoplates prepared by using different soft templates possessed typical porous hexagonal layered structure. Many spherical pores were uniformly distributed on the surfaces of the $Co(OH)_2$-F nanoplates (synthesized by using F127), which were much smaller than that formed on the $Co(OH)_2$-P nanoplates (synthesized by using P123). It was considered that different sizes of composite micelles were produced during the reaction resulting in the generation of different sizes of pores on $Co(OH)_2$. However, without the soft templates, $Co(OH)_2$ nanoplates have no obvious porous structure (Fig. 1c), indicating the important role of soft

View Article Online
DOI: 10.1039/C8NR06162A

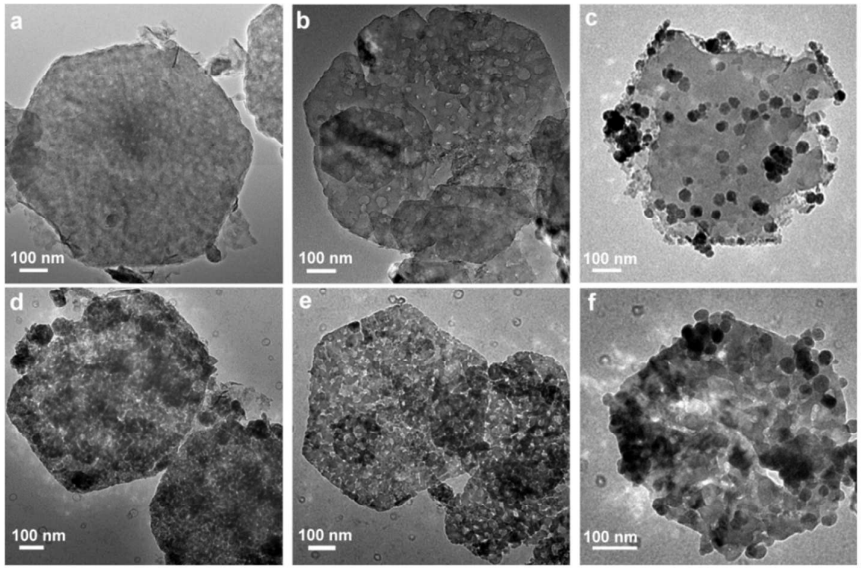

Fig. 1 TEM images of $Co(OH)_2$-F (a), $Co(OH)_2$-P (b), $Co(OH)_2$ (c), Co_3O_4-F (d), Co_3O_4-P (e) and Co_3O_4 (f).

template on the preparation of porous $Co(OH)_2$ nanoplates. After annealing at 450 °C in air, $Co(OH)_2$ nanoplates were transformed into Co_3O_4 nanoplates. Simultaneously, some mesopores were generated in Co_3O_4 due to the escape of water in the decomposition of $Co(OH)_2$ [eq.2]. As shown in the TEM images (Fig. 1d, 1e and 1f), the obtained Co_3O_4 reserved the porous hexagonal nanoplate shape and had a similar size to the $Co(OH)_2$ precursor. SEM images (Fig. S1) also gave the same conclusions. Nitrogen adsorption/desorption experiments were conducted to determine the specific surface area and porous properties of Co_3O_4 nanoplates (Fig. S2). The obtained Co_3O_4-F possessed the smallest Barrett-Joyner-Halenda (BJH) mean pore size (3.06 nm) and the largest pore volume (0.62 $cm^3\ g^{-1}$). The average Brunauer-Emmett-Teller (BET) surface area of Co_3O_4-F is 244.4 $m^2\ g^{-1}$, which was much larger than that of Co_3O_4-P (192.6 $m^2\ g^{-1}$) and Co_3O_4 (168.2 $m^2\ g^{-1}$). These results further confirm the remarkable small and denser porous structure of Co_3O_4-F nanoplates.

$$[Co(H_2O)_6]^{2+} + 2NH_3 \cdot H_2O \rightarrow Co(OH)_2 \downarrow + 2NH_4^+ + 6H_2O \quad (1)$$

$$6Co(OH)_2 + O_2 \rightarrow 2Co_3O_4 + 6H_2O \uparrow \quad (2)$$

Powder XRD was performed to confirm the phases of the as-synthesized nanoplates. As shown in Fig. 2a, the XRD patterns of $Co(OH)_2$-F, $Co(OH)_2$-P and $Co(OH)_2$ matched well with the standard file of β-$Co(OH)_2$ (JCPDS card #30-443). The strongest (001) diffraction peak suggested a preferred growth of β-$Co(OH)_2$ with (001) facets, and the other impurity phases were not found indicating the good crystallinity of the products. The XRD patterns of Co_3O_4-F, Co_3O_4-P and Co_3O_4 (Fig. 2b) matched well with the standard file of Co_3O_4 (JCPDS card #43-1003), demonstrated that $Co(OH)_2$ was successfully transformed into Co_3O_4 after the annealing process.

Switchable peroxidase- and catalase-like activity of Co_3O_4-F

To investigate the peroxidase-like activity of porous Co_3O_4-F nanoplates, the catalysis of typical peroxidase substrate 3,3',5,5'-tetramethylbenzidine (TMB) was tested in the presence of H_2O_2. As shown in Fig. 3a, Co_3O_4-F could catalyze the oxidation of TMB to produce the blue color in the presence of H_2O_2. However, only with Co_3O_4-F or H_2O_2, TMB could hardly be oxidized, indicating the intrinsic peroxidase-like activity of Co_3O_4-F. Then, the catalytic activities of Co_3O_4, Co_3O_4-P and Co_3O_4-F were compared to study the influence of morphology

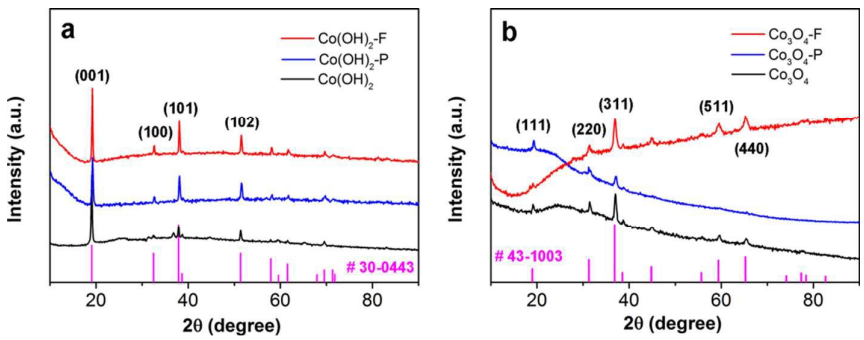

Fig. 2 (a) XRD patterns of $Co(OH)_2$-F, $Co(OH)_2$-P and $Co(OH)_2$, (b) XRD patterns of Co_3O_4-F, Co_3O_4-P and Co_3O_4.

View Article Online
DOI: 10.1039/C8NR06162A

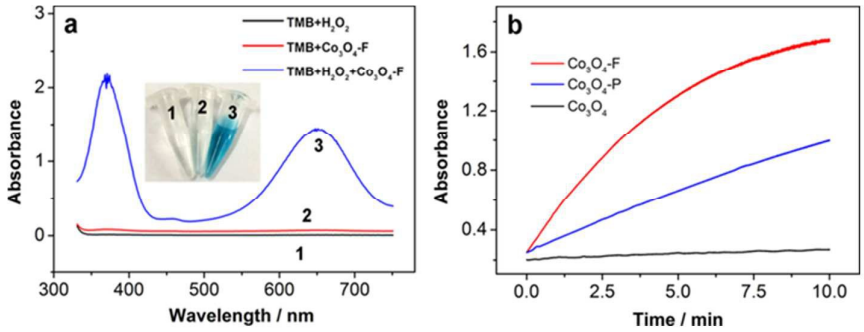

Fig. 3 (a) The absorption spectra and digital photos of different colorimetric reaction systems: (1) TMB+H_2O_2, (2) TMB+Co_3O_4-F, and (3) TMB+H_2O_2+Co_3O_4-F. (b) Time-dependent absorbance changes at 652 nm of TMB using different catalysts. Reaction conditions: 0.25 mM TMB, 3 mM H_2O_2 and 10 μg mL^{-1} Co_3O_4-F were incubated in 0.1 M HAc-NaAc buffer (pH 6.0) for 10 min.

on their peroxidase mimetic properties. It can be seen in Fig. 3b, Co_3O_4 synthetized without soft templates had little catalytic activity and the catalytic activity of Co_3O_4-F was much higher than that of Co_3O_4-P. The smaller and denser pore structure of Co_3O_4-F nanoplates could provide a larger surface area with active sites for the catalytic reaction, enhancing the catalytic efficiency. Therefore, Co_3O_4-F was chosen for the subsequent experiments.

It was interested that many gas bubbles were observed when Co_3O_4-F was added into the tubes containing H_2O_2 under the basic conditions, suggesting that Co_3O_4-F also exhibited the intrinsic CAT-like activity. Co_3O_4-F could catalyze the decomposition of H_2O_2 into oxygen and water similarly like CAT. The effects of pH and temperature on the dual enzyme mimetic activity of Co_3O_4-F were studied as shown in Fig. 4. When incubated in HAc-NaAc buffer at room temperature (25 °C), Co_3O_4-F exhibited the highest peroxidase-like catalytic activity at pH 6.0 (Fig. 4a, red curve), unlike most of other peroxidase mimics whose optimal reaction conditions were pH 4.0.[4, 5, 23, 32] With the temperature increasing, the optimal pH for Co_3O_4-F changed to acidic conditions (pH 4.0) while the peroxidase-like catalytic activity reduced sharply at pH 6.0. At 4 °C, Co_3O_4-F exhibited good catalytic activity in neutral pH. However, the situations have changed for Co_3O_4-F as CAT mimic. As shown in Fig. 4b, the bubbles grew faster and bigger with the pH and temperature increasing. At 50 °C, we could even observe the gas bubbles at the acid conditions. It could be concluded that Co_3O_4-F would like to exhibited CAT-like activity under the condition of high temperature and basic solutions in the investigated range.

In the catalytic activity analysis, the apparent activation energy (Ea) of Co_3O_4-F as peroxidase mimic or CAT mimic was evaluated based on reaction rates (k) measured at different temperatures from 18 °C to 50 °C. As shown in Fig. S3, the value of k could be obtained through monitoring absorbance change of the corresponding substrates (Fig. S3a and S3b) and fitting the absorbance data to pseudo-first-order kinetics (Fig. S3c and S3d). We could find that the rate constant increased with increasing temperature and the value of k for peroxidase-like pathway was higher than that for CAT-like pathway, indicating that the oxidation reaction of TMB went faster than the decomposition of H_2O_2 catalyzed by Co_3O_4-F. According to the Arrhenius equation, the activation energy for these two pathways was determined from the slope of the linear regression as shown in Fig. 5a. The activation energy of peroxidase-like pathway was 26.06 kJ mol^{-1}, which was lower than that of CAT-like pathway (59.94 kJ mol^{-1}), suggesting a higher temperature sensitivity for the CAT-like activity of

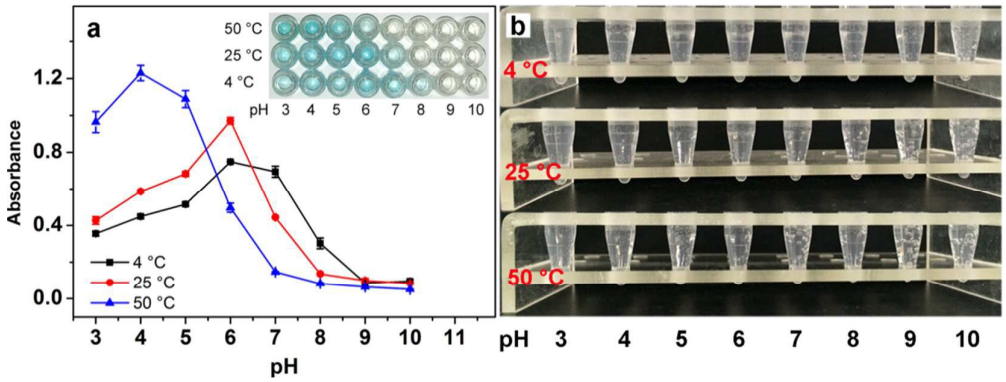

Fig. 4 (a) Peroxidase-like activities of Co_3O_4-F depended on pH and temperature. Reaction conditions: 0.25 mM TMB, 3 mM H_2O_2 and 5 μg mL^{-1} Co_3O_4-F were incubated in 0.1 M HAc-NaAc buffer for 10 min for absorbance spectroscopy measurement. (b) CAT-like activities of Co_3O_4-F depended on pH and temperature. Reaction conditions: 20 μg mL^{-1} Co_3O_4-F and 10 mM H_2O_2 were incubated in 0.1 M HAc-NaAc buffer for 30 min.

View Article Online
DOI: 10.1039/C8NR06162A

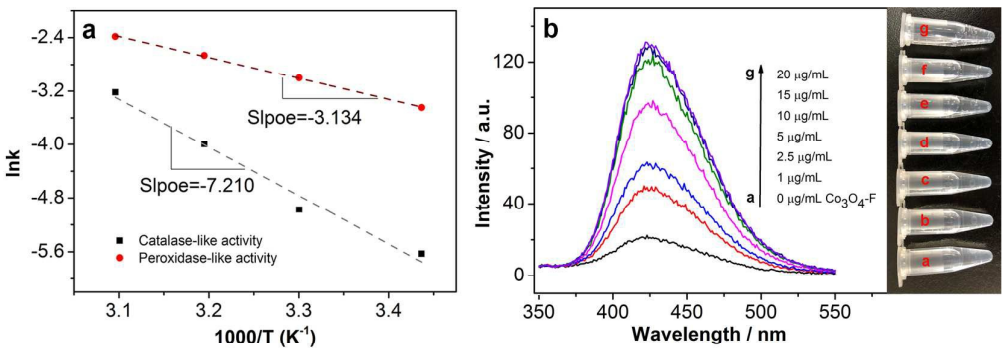

Fig. 5 (a) Arrhenius plot for the reactions catalyzed by Co_3O_4-F. (b) The effect of Co_3O_4-F on the formation of hydroxyl radical with terephthalic acid as a fluorescence probe. Reaction conditions: 0.625 mM terephthalic acid, 50 mM H_2O_2 and different concentrations of Co_3O_4-F were incubated in 0.1 M HAc-NaAc buffer (pH 6.0) for 3 h.

Co_3O_4-F.

To better understand the process of the catalytic reaction, •OH was assessed by adding the fluorescent probe terephthalic acid into the H_2O_2-Co_3O_4-F system, where highly fluorescent 2-hydroxy terephthalic acid was generated by the strong interaction between terephthalic acid and •OH radical.[33] As shown in Fig. 5b, the fluorescence intensity was weak when there was no Co_3O_4-F. Nevertheless, the increase of the fluorescence intensity was observed when the concentration of Co_3O_4-F increased to 10 μg mL^{-1}. However, when the concentration of Co_3O_4-F continued to increase the fluorescence intensity reached a platform indicating that no more•OH radical was formed. Meanwhile, many gas bubbles were observed in the tubes suggesting that high concentration of Co_3O_4-F would like to catalyze the decomposition of H_2O_2 into oxygen and water as CAT mimic.

As a result, porous Co_3O_4-F nanoplates possessed dual enzyme-like activity which could be switched by pH. With the temperature changing, both of the activity and the switch pH for dual enzyme mimetic activity have changed. The possible mechanism of Co_3O_4-F possessed peroxidase- and CAT-like activity was considered to be like the reported works.[3, 12, 34-36] Briefly, porous Co_3O_4-F nanoplates can catalyze H_2O_2 to produce •OH, exhibiting peroxidase-like catalytic activity. Under the high temperature, basic solutions or with high concentration of Co_3O_4-F, O_2^{2-} was generated simultaneously in large amounts, accompanied by a substantial release of O_2, exhibiting as CAT mimic. Peroxidase and CAT have wide practical applications in biosensing and nanomedicine. Therefore, it is of great significance to accurately control the activity and the switch conditions of nanozymes with multi-enzyme mimetic activity.

Peroxidase-like activity of Co_3O_4-F and its applications in detecting glucose

Afterwards, we adopted pH 6.0 and 25 °C for the subsequent analysis of Co_3O_4-F peroxidase-like catalytic activity. The apparent steady-state kinetic parameters were obtained by varying one substrate concentration while keeping the other substrate concentration constant. It is obvious that the oxidation reaction catalyzed by Co_3O_4-F followed the typical Michaelis-Menten behavior towards both substrates, TMB and H_2O_2 (Fig. S4a and S4c). The Michaelis-Menten constant (K_m) and the maximum initial velocity (V_m) given in Table S1 could be calculated by using Lineweaver-Burk plot (Fig. S4b and S4d). Compared with HRP[1] and the other reported nanozymes,[5] the K_m value of the porous Co_3O_4-F nanoplates with TMB or H_2O_2 as the substrate is lower, suggesting that Co_3O_4-F have a higher affinity to TMB and H_2O_2. Due to the presence of porous structure, Co_3O_4-F have a better catalytic property than

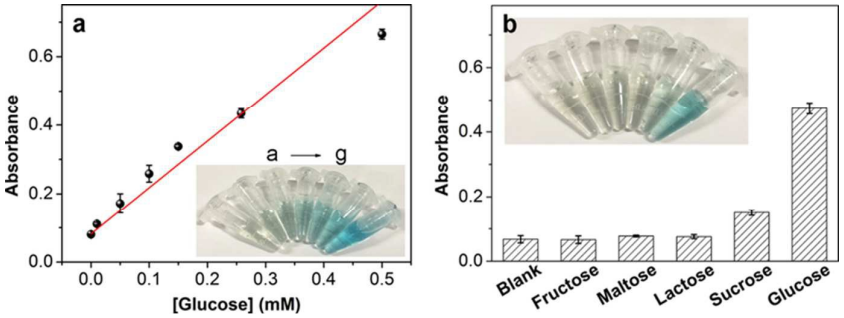

Fig. 6 (a) The absorption spectra of TMB with different glucose concentrations from a to g: 0, 0.01, 0.05, 0.1, 0.2, 0.3 and 0.5 mM). (b) The selectivity of glucose detection (from left to right: blank, 3 mM fructose, 3 mM maltose, 3 mM lactose, 3 mM sucrose and 0.3 mM glucose). Inset: the color change with the different solutions. The error bars represent the standard deviation of three measurements.

View Article Online
DOI: 10.1039/C8NR06162A

the reported Co_3O_4 NPs.[35]

Based on the good peroxidase-like activity of Co_3O_4-F, a simple and sensitive colorimetric glucose biosensor could be developed by combining glucose oxidase (GOx) because H_2O_2 is the main product of GOx-catalyzed reaction.[37, 38] More importantly, GOx maintained good catalytic activity at the optimal reaction condition for Co_3O_4-F (pH 6.0, 25 °C). The traditional two-step colorimetric glucose biosensing based on peroxidase mimic was successfully combined into one-step, making the operation simpler and easier. As shown in Fig. 6a, the color of the corresponding solution gradually changed from colorless to deep blue as the glucose concentration increased. There is a good linear relationship between the absorbance at 652 nm and the glucose concentration in the range of 0.01-0.5 mM with a detection limit of 9.7 μM. In addition, fructose, maltose, lactose and sucrose were used to test the specificity of the colorimetric sensor. Even when the concentration of the control samples was 10 times higher than glucose, the glucose could be easily distinguished by the naked eye (Fig. 6b), indicating the good selectivity of the constructed glucose biosensor. Using this method, we detected glucose in 50-fold dilution fetal bovine serum, and the results are listed in Table S2. According to the calibration curve, the recoveries of glucose fall in the range of 91.2-94.0 % by using the standard addition method, indicating that this Co_3O_4-F based colorimetric method is applicable to determining glucose in real samples.

Conclusions

In summary, we have synthesized porous Co_3O_4 nanoplates with different pore sizes by using different soft templates F127 and P123. Co_3O_4-F exhibited the highest peroxidase-like catalytic activity due to the uniform small pore structure. Also, porous Co_3O_4-F nanoplates possessed excellent CAT-like property under the basic conditions. By adjusting the temperature and pH, the dual enzyme-like activity could be switched and simultaneously regulated. It is very important and challenging to flexibly control the multi-enzyme mimetic catalytic properties of nanomaterials according to the conditions of the practical applications. Then, a simple one-step colorimetric glucose biosensor has been constructed based on the peroxidase-like activity of Co_3O_4-F, simplifying the operation and providing a new strategy for the construction of glucose sensors.

Conflicts of interest

The authors declare no competing financial interests.

Acknowledgements

This work was supported by the National Natural Science Foundation of China (Nos. 21375123 and 21675151) and the Ministry of Science and Technology of China (Nos. 2013YQ170585 and 2016YFA0203201)

Notes and references

1 L. Z. Gao, J. Zhuang, L. Nie, J. B. Zhang, Y. Zhang, N. Gu, T. H. Wang, J. Feng, D. L. Yang, S. Perrett and X. Yan, *Nat. Nanotechnol.*, 2007, **2**, 577-583.
2 Z. Zhu, Y. Zhai, C. Zhu, Z. Wang and S. Dong, *Electrochem. Commun.*, 2013, **36**, 22-25.
3 Q. Wang, L. Zhang, C. Shang, Z. Zhang and S. Dong, *Chem. Commun.*, 2016, **52**, 5410-5413.
4 H. Wei and E. Wang, *Anal. Chem.*, 2008, **80**, 2250-2254.
5 L. Zhang, L. Han, P. Hu, L. Wang and S. Dong, *Chem. Commun.*, 2013, **49**, 10480-10482.
6 Y. Wang, Y. Zhu, A. Binyam, M. Liu, Y. Wu and F. Li, *Biosens. Bioelectron.*, 2016, **86**, 432-438.
7 K. Wang, D. Feng, T.-F. Liu, J. Su, S. Yuan, Y.-P. Chen, M. Bosch, X. Zou and H.-C. Zhou, *J. Am. Chem. Soc.*, 2014, **136**, 13983-13986.
8 Y. Guo, L. Deng, J. Li, S. Guo, E. Wang and S. Dong, *ACS Nano*, 2011, **5**, 1282-1290.
9 L. Deng, C. Chen, C. Zhu, S. Dong and H. Lu, *Biosensors & Bioelectronics*, 2014, **52**, 324-329.
10 X. Shen, W. Liu, X. Gao, Z. Lu, X. Wu and X. Gao, *J. Am. Chem. Soc.*, 2015, **137**, 15882-15891.
11 J. Mu, Y. Wang, M. Zhao and L. Zhang, *Chem. Commun.*, 2012, **48**, 2540-2542.
12 L. Su, W. Qin, H. Zhang, Z. U. Rahman, C. Ren, S. Ma and X. Chen, *Biosens. Bioelectron.*, 2015, **63**, 384-391.
13 W. Li, Z. Liu, C. Liu, Y. Guan, J. Ren and X. Qu, *Angew. Chem. Int. Ed.*, 2017, **56**, 13661-13665.
14 Y. Huang, Z. Liu, C. Liu, E. Ju, Y. Zhang, J. Ren and X. Qu, *Angew. Chem. Int. Ed.*, 2016, **55**, 6646-6650.
15 N. Singh, M. A. Savanur, S. Srivastava, P. D'Silva and G. Mugesh, *Angew. Chem. Int. Ed.*, 2017, **56**, 14267-14271.
16 J. Chen, S. Patil, S. Seal and J. F. McGinnis, *Nat. Nanotechnol.*, 2006, **1**, 142.
17 Y. Li, X. He, J.-J. Yin, Y. Ma, P. Zhang, J. Li, Y. Ding, J. Zhang, Y. Zhao, Z. Chai and Z. Zhang, *Angew. Chem. Int. Ed.*, 2015, **54**, 1832-1835.
18 C. Korsvik, S. Patil, S. Seal and W. T. Self, *Chem. Commun.*, 2007, DOI: 10.1039/B615134E, 1056-1058.
19 A. A. Vernekar, T. Das and G. Mugesh, *Angewandte Chemie*, 2016, **128**, 1434-1438.
20 H. Cheng, S. Lin, F. Muhammad, Y.-W. Lin and H. Wei, *ACS Sensors*, 2016, **1**, 1336-1343.
21 A. Asati, C. Kaittanis, S. Santra and J. M. Perez, *Anal. Chem.*, 2011, **83**, 2547-2553.
22 R. Pautler, E. Y. Kelly, P.-J. J. Huang, J. Cao, B. Liu and J. Liu, *ACS Appl. Mat. Interfaces*, 2013, **5**, 6820-6825.
23 H. Zhao, Y. Dong, P. Jiang, G. Wang and J. Zhang, *ACS Appl. Mat. Interfaces*, 2015, **7**, 6451-6461.
24 T. Pirmohamed, J. M. Dowding, S. Singh, B. Wasserman, E. Heckert, A. S. Karakoti, J. E. S. King, S. Seal and W. T. Self, *Chem. Commun.*, 2010, **46**, 2736-2738.
25 B. Liu, Z. Sun, P.-J. J. Huang and J. Liu, *J. Am. Chem. Soc.*, 2015, **137**, 1290-1295.
26 C. Xu and X. Qu, *Npg Asia Materials*, 2014, **6**, e90.
27 W. Zhang, Y. Shi, Y. Chen, J. Ye, X. Sha and X. Fang, *Biomaterials*, 2011, **32**, 2894-2906.
28 A. R. Fares, A. N. ElMeshad and M. A. A. Kassem, *Drug Delivery*, 2018, **25**, 132-142.
29 Y. Huang, H. Cai, D. Feng, D. Gu, Y. Deng, B. Tu, H. Wang, P. A. Webley and D. Zhao, *Chem. Commun.*, 2008, DOI: 10.1039/B804716B, 2641-2643.
30 B. Jiang, C. Li, M. Imura, J. Tang and Y. Yamauchi, *Advanced Science*, 2015, **2**, 1500112-n/a.
31 B.-R. Jia, M.-L. Qin, S.-M. Li, Z.-L. Zhang, H.-F. Lu, P.-Q. Chen, H.-Y. Wu, X. Lu, L. Zhang and X.-H. Qu, *ACS Appl. Mat. Interfaces*, 2016, **8**, 15582-15590.

View Article Online
DOI: 10.1039/C8NR06162A

32 Q. Wang, X. Zhang, L. Huang, Z. Zhang and S. Dong, *ACS Appl. Mat. Interfaces*, 2017, **9**, 7465-7471.
33 K.-i. Ishibashi, A. Fujishima, T. Watanabe and K. Hashimoto, *J. Photochem. Photobiol., A*, 2000, **134**, 139-142.
34 K. Sobańska, P. Pietrzyk and Z. Sojka, *ACS Catalysis*, 2017, **7**, 2935-2947.
35 J. Dong, L. Song, J.-J. Yin, W. He, Y. Wu, N. Gu and Y. Zhang, *ACS Appl. Mat. Interfaces*, 2014, **6**, 1959-1970.
36 J. Li, W. Liu, X. Wu and X. Gao, *Biomaterials*, 2015, **48**, 37-44.
37 Q. Wang, H. Wei, Z. Zhang, E. Wang and S. Dong, *TrAC, Trends Anal. Chem.*, 2018, **105**, 218-224.
38 Q. Wang, X. Zhang, L. Huang, Z. Zhang and S. Dong, *Angew. Chem. Int. Ed.*, 2017, **56**, 16082-16085.

View Article Online
DOI: 10.1039/C8NR06162A

TOC

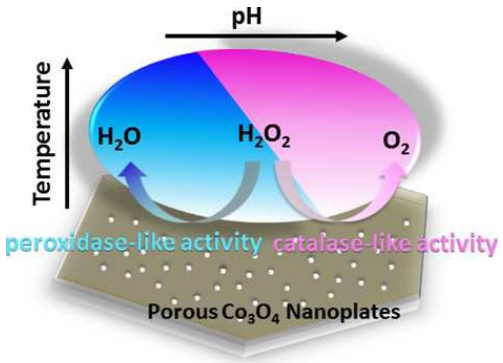

The as-prepared porous Co_3O_4 nanoplates possessed both of peroxidase and catalase mimetic activities, which could be switched by pH.